nature plants

Letter

https://doi.org/10.1038/s41477-022-01279-8

# Targeted A-to-G base editing of chloroplast DNA in plants

Received: 23 July 2022

Accepted: 19 October 2022

Published online: 1 December 2022

Check for updates

Young Geun Mok[1,3,4], Sunghyun Hong[1,3,4], Su-Ji Bae[1], Sung-Ik Cho[1,2] & Jin-Soo Kim[1,3]

Chloroplast DNA (cpDNA) encodes up to 315 (typically, 120–130) genes[1], including those for essential components in photosystems I and II and the large subunit of RuBisCo, which catalyses $CO_2$ fixation in plants. Targeted mutagenesis in cpDNA will be broadly useful for studying the functions of these genes in molecular detail and for developing crops and other plants with desired traits. Unfortunately, CRISPR–Cas9 and CRISPR-derived base editors, which enable targeted genetic modifications in nuclear DNA, are not suitable for organellar DNA editing[2], owing to the difficulty of delivering guide RNA into organelles. CRISPR-free, protein-only base editors (including DddA-derived cytosine base editors[3–8] and zinc finger deaminases[9]), originally developed for mitochondrial DNA editing in mammalian cells, can be used for C-to-T, rather than A-to-G, editing in cpDNA[10–12]. Here we show that heritable homoplasmic A-to-G edits can be induced in cpDNA, leading to phenotypic changes, using transcription activator-like effector-linked deaminases[13].

To demonstrate targeted A-to-G editing in plant organelles using transcription activator-like effector (TALE)-linked deaminases (TALEDs), which are composed of custom-designed TALE DNA-binding arrays, split $DddA_{tox}$ originating from *Burkholderia cenocepacia* and an engineered deoxyadenosine deaminase (TadA-8e) derived from the *Escherichia coli* TadA protein, we first chose three chloroplast genes (*rrn16*, *psbA* and *psaA*) in lettuce (*Lactuca sativa*) (Fig. 1a and Extended Data Fig. 1). Mutations in these genes give rise to resistance to antibiotics (*rrn16* encoding 16S ribosomal RNA)[14] or herbicide (*psbA*)[15] and to an albino phenotype (*psaA*)[12]. We co-transfected in vitro transcripts (mRNA) encoding TALEDs with a plastid transit peptide (PTP) of the *Arabidopsis* RecA1 protein into lettuce protoplasts and measured base editing frequencies using targeted deep sequencing at day 7 post-transfection (Fig. 1b–g). As expected, two TALED pairs (L–1397N (left-side TALE fused to the amino-terminal half of $DddA_{tox}$ split at Gly1397) + R–1397C–AD (right-side TALE fused to the carboxy-terminal half of $DddA_{tox}$ split at Gly1397 and the TadA-8e adenine deaminase) and L–1397C–AD + R–1397N) targeted to the *rrn16* site induced A-to-G conversions with editing frequencies of up to 46% without causing C-to-T conversions (Fig. 1b,c). Adenines in the spacer region between the two TALE-binding sites were edited more efficiently than those positioned outside the region. Two TALED pairs (L–1397N + R–1397C–AD and L–1397C–AD + R–1397N) targeted to the *psbA* site also induced A-to-G conversions with editing frequencies of up to 25%. Bystander A-to-G edits (A-26) were also induced outside of the spacer region with a frequency of 21% by the L–1397N + R–1397C–AD pair (Fig. 1d), which could have been caused by relatively poor affinity of the left-side TALE array (L) for the target DNA. At the *psaA* target site, two TALED pairs (L–1397N + R–1397C–AD and L–1397C–AD + R–1397N) induced A-to-G conversions in lettuce protoplasts with editing frequencies of up to 51% (Fig. 1f). Unexpectedly, C-to-T conversions (C2) were also induced with up to 3.5% efficiencies (Fig. 1f), suggesting that uracil-glycosylase-inhibitor-free split TALEDs could induce C-to-T edits in addition to A-to-G edits (albeit less efficiently) in chloroplasts, unlike in mammalian mitochondria.

We next chose three *Arabidopsis* chloroplast genes (*psaA*, *rbcL* and *rrn16S*) to investigate whether TALED-mediated edits in chloroplast DNA (cpDNA) could be stably maintained in whole plants. We obtained

[1]Center for Genome Engineering, Institute for Basic Science, Daejeon, Republic of Korea. [2]Department of Chemistry, Seoul National University, Seoul, Republic of Korea. [3]Present address: GreenGene Inc., Seoul, Republic of Korea. [4]These authors contributed equally: Young Geun Mok, Sunghyun Hong. e-mail: jskim01@snu.ac.kr

https://doi.org/10.1038/s41477-022-01279-8

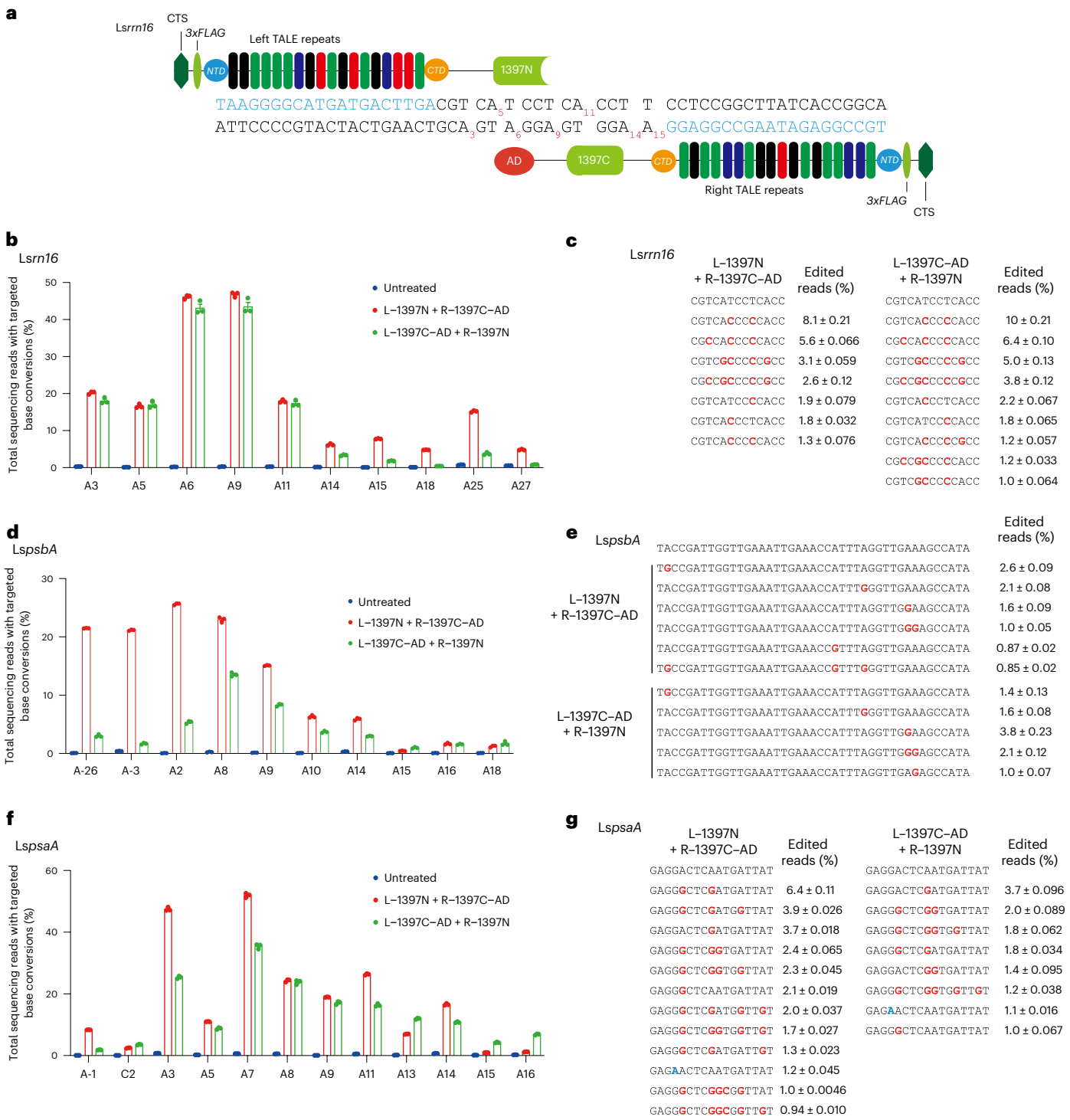


**Fig. 1 | TALED-mediated cpDNA editing in lettuce protoplasts. a**, TALED pairs designed to target the *rrn16* chloroplast gene in lettuce (*Ls*). The TALE-binding sites are shown in blue. CTS, chloroplasts target signal; NTD, N-terminal domain; CTD, C-terminal domain. **b**–**g**, Frequencies of base conversions and edited alleles induced by TALEDs in *rrn16* (**b**,**c**), *psbA* (**d**,**e**) and *psaA* (**f**,**g**). A-to-G and C-to-T edited bases are shown in red and blue, respectively (**c**,**e**,**g**). The error bars show the standard error of the mean (±s.e.m.) for three biologically independent experiments.

T1 transformants using a transfer DNA binary vector encoding a TALED pair specific to each gene under the control of the *RPS5A* promoter and the 35S terminator[11] (Extended Data Fig. 2). Targeted deep sequencing showed that A-to-G base editing was induced at multiple positions with frequencies of up to 99% in 16 of 20 T1 plants transformed with the *psaA*-targeted TALED pair (Extended Data Fig. 3a). Among the 16 edited transformants, 15 plants had mutations that disrupted the start codon (A8 and A9, underlined in Fig. 2a). As a result, seven transformants showed an albino phenotype to varying degrees. Two plantlets with almost complete albino phenotypes failed to grow (Extended Data Fig. 3b). As shown with lettuce protoplasts (Fig. 1f,g), C-to-T conversions were also observed, with editing frequencies of up to 98% (#2, C2) in these T1 plants (Extended Data Fig. 3c). Interestingly, unlike *psaA* T1 #1 and #2 plants showing a wild-type morphology without an albino

https://doi.org/10.1038/s41477-022-01279-8

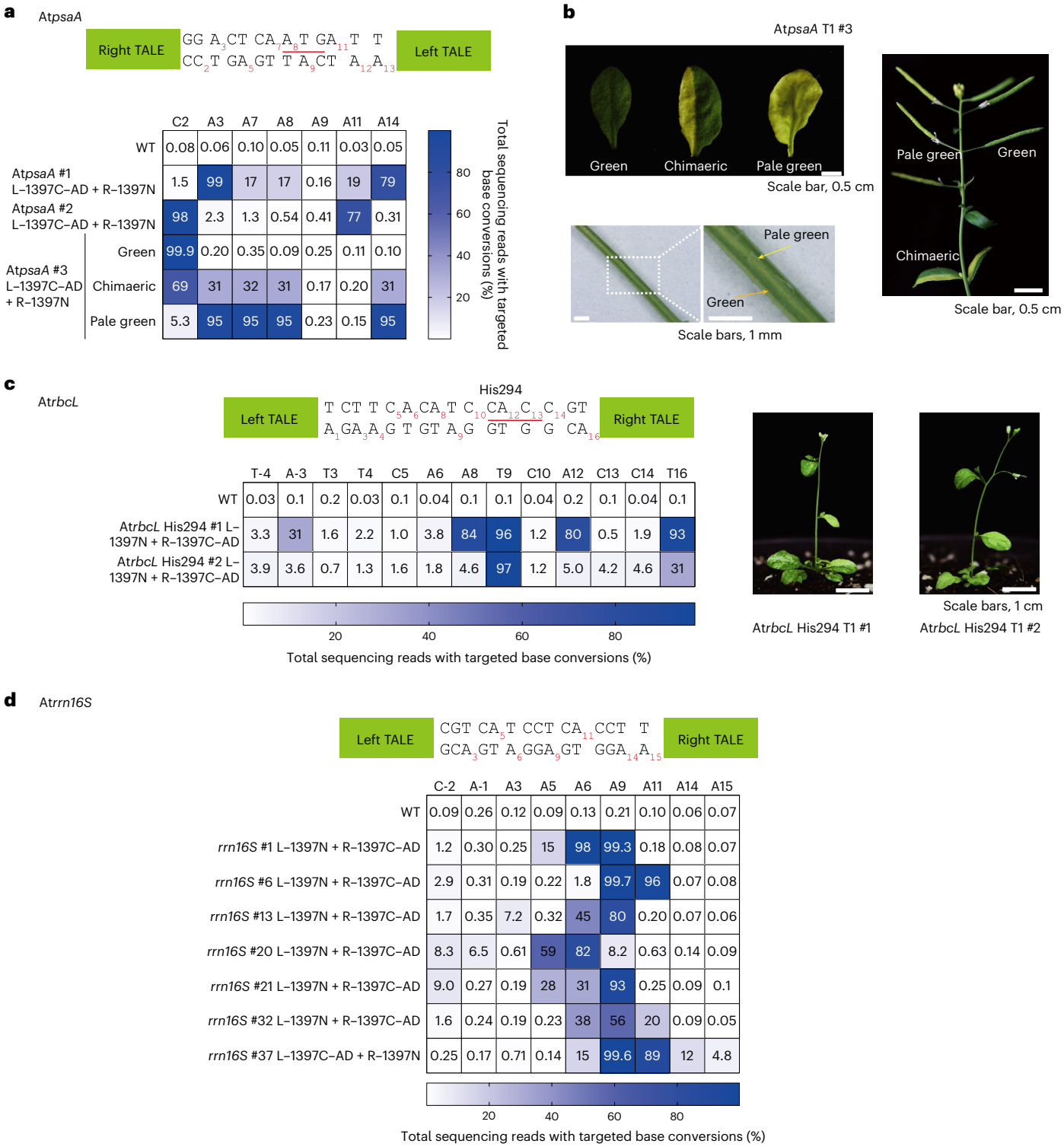


**Fig. 2 | TALED-mediated cpDNA editing in *Arabidopsis*.** **a**–**d**, Heat maps showing editing frequencies and phenotypes of *Arabidopsis* T1 plants expressing TALEDs targeted to *psaA* (**a**,**b**), *rbcL* (**c**) and *rrn16S* (**d**). The TALE-binding regions are shown in green. The start codon in *psaA* (**a**) and the codon for His294 in *rbcL* (**c**) are underlined. WT, wild type.

phenotype, the *psaA* T1 #3 plant was mosaic, with green, chimaeric and pale-green leaves. Pale-green traits were also observed in stems and siliques (Fig. 2b). In particular, the editing frequencies of an adenine (A8) in the start codon were 0.1%, 31% and 95% in green, chimaeric and pale-green leaves, suggesting that albinism was caused by the disruption of the *psaA* gene via adenine base editing (Fig. 2a,b). The other five chimaeric T1 plants (#16–20) also showed A-to-G conversions at this position (A8), with frequencies that ranged from 52% to 78% (Extended Data Fig. 3a). Two T1 (#9 and #10) plantlets with the highest editing frequencies (97% and 99%) at this position died prematurely. These results demonstrate that nearly homoplasmic (~99%) adenine editing can be obtained in *Arabidopsis* T1 transformants using TALEDs expressed under the control of the *RPSSA* promoter, which is active at an early embryonic stage in meristem regions[16].

https://doi.org/10.1038/s41477-022-01279-8

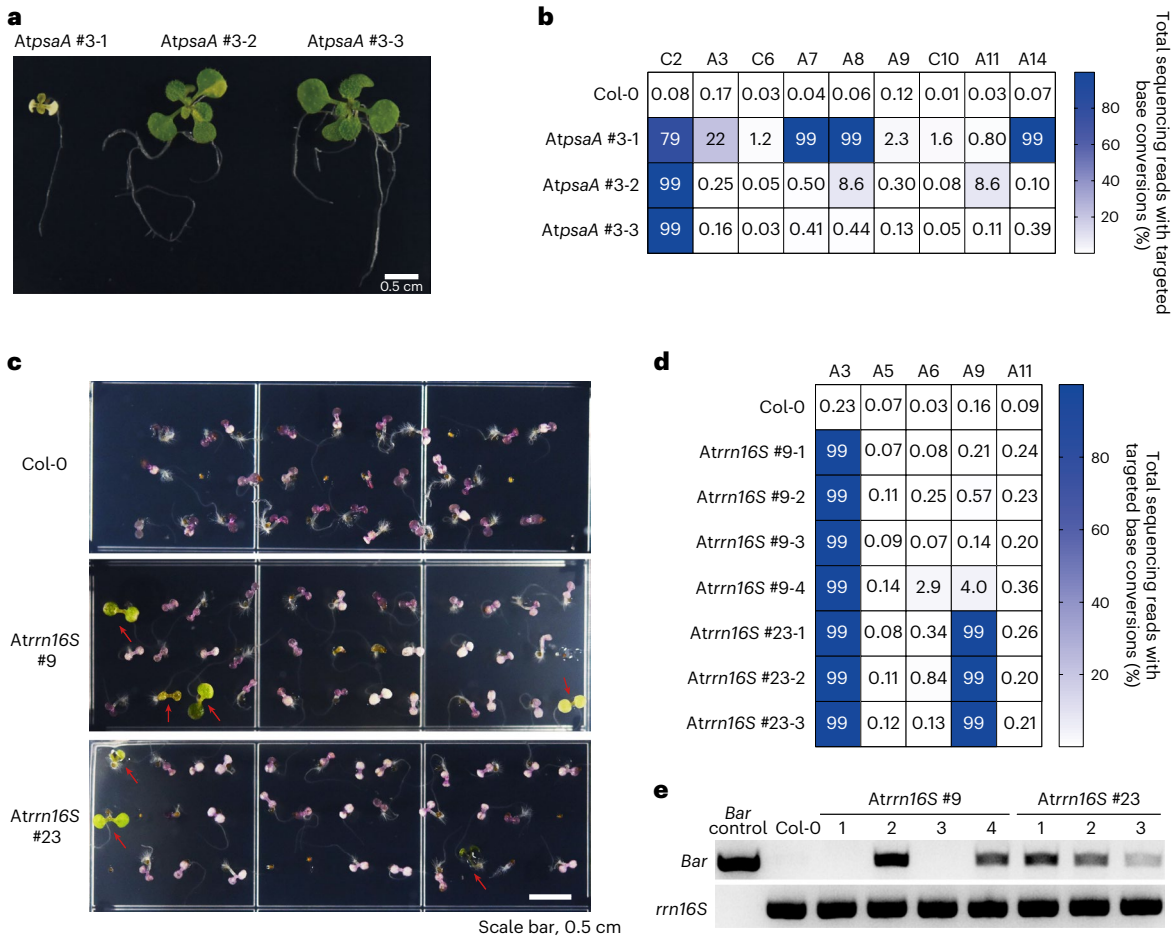


**Fig. 3 | Phenotypes and genotypes of *Arabidopsis* T2 plants. a**, Two-week-old T2 seedlings from the #3 *psaA*-edited T1 plant grown on half-strength MS medium containing 1% sucrose under long-day conditions. **b**, Base-editing frequencies of T2 progenies. **c**, One-week-old Col-0 and T2 seedlings from At*rrn16S*-edited T1 plants (#9 and #23) grown on half-strength MS medium containing 1% sucrose and spectinomycin (10 mg $l^{-1}$) under long-day conditions. The red arrows indicate spectinomycin-resistant seedlings. **d**, Base-editing frequencies of spectinomycin-resistant At*rrn16S*-edited T2 progenies. **e**, PCR amplification of the Bar transgene (552 base pairs) in genomic DNA isolated from spectinomycin-resistant T2 seedlings. *rrn16S* (235 base pairs) was used as an internal control.

We next analysed *rbcL*-targeted T1 plants. The *rbcL* gene encodes the large, catalytic subunit of RuBisCo, the enzyme catalysing $CO_2$ fixation in chloroplasts[1]. A-to-G conversions were induced at several positions in the spacer region with editing frequencies of up to 99.3% in a total of six T1 transformants with chimaeric leaves (Fig. 2c and Extended Data Fig. 4). C-to-T conversions were rarely induced at two positions in a 5′-TC-3′ context (C5 and C10) in these plants. These mutations gave rise to alterations in amino acid sequences around His294 (underlined in Fig. 2c), an amino acid residue absolutely conserved among all members of the RuBisCo superfamily. Apparently, the resulting RuBisCo proteins were poorly active, resulting in partial albinism. In addition, we obtained a total of 37 T1 plants with the *rrn16S*-targeted TALED. Among these, 35 plants were base edited with frequencies that ranged from 1.3% to 99.8% (Fig. 2d and Extended Data Fig. 5), demonstrating that homoplasmic mutations can be induced in whole plants using TALEDs.

Next, we investigated whether TALED-induced edits in cpDNA were inherited in the next generation. We harvested T2 seeds from the #3 *psaA*-edited T1 plant and grew T2 progenies on half-strength Murashige and Skoog (MS) media under long-day (16 h of light and 8 h of dark) conditions for 14 days to confirm phenotypic alterations. Interestingly, T2 plants showed diverse phenotypes and genotypes (Fig. 3a,b). Targeted deep sequencing showed that A8 in the start codon was almost completely (99%), partially (8.6%) and poorly (0.44%) edited in albino (#3-1), chimaeric (#3-2) and wild-type-like (#3-3) plants, respectively (Fig. 3b), suggesting that the disruption of the initiation codon gave rise to albinism. Furthermore, we were able to obtain spectinomycin-resistant plants after T2 seeds of *rrn16S*-edited T1 lines were sown in half-strength MS medium containing spectinomycin, an antibiotic that inhibits protein synthesis (Fig. 3c). Interestingly, A3, which had been minimally edited in T1 plants with an average editing frequency of 0.47 ± 0.19%, was almost completely (99%) converted to guanine in several T2 plants resistant to spectinomycin (Fig. 3d). No other mutations, in addition to A3-to-G conversions, were induced at >1.0% frequencies in a total of 13 spectinomycin-resistant, *rrn16S*-edited #9 T2 lines (Extended Data Fig. 6), suggesting that A3 editing was responsible for the drug resistance. We also found that two spectinomycin-resistant T2 plants (#9-1 and 3) were transgene-free (Fig. 3e), indicating that the A3-to-G edit was induced in T1 plants and that the insertion of multiple copies of transgene is not required to induce homoplasmic editing. Note also that transgene-free, cpDNA-edited plants can be exempt from genetically modified organism regulations[17,18]. Taken together, these results demonstrate that base edits induced by TALEDs in cpDNA are transmitted to the next generation.

Last, we profiled the off-target activity of the TALEDs targeted to the *psaA* and *rrn16S* sites in T1 plants using whole-genome sequencing (Fig. 4). We were able to confirm on-target edits in each sample and to identify several A-to-G or C-to-T mutations with low conversion

https://doi.org/10.1038/s41477-022-01279-8

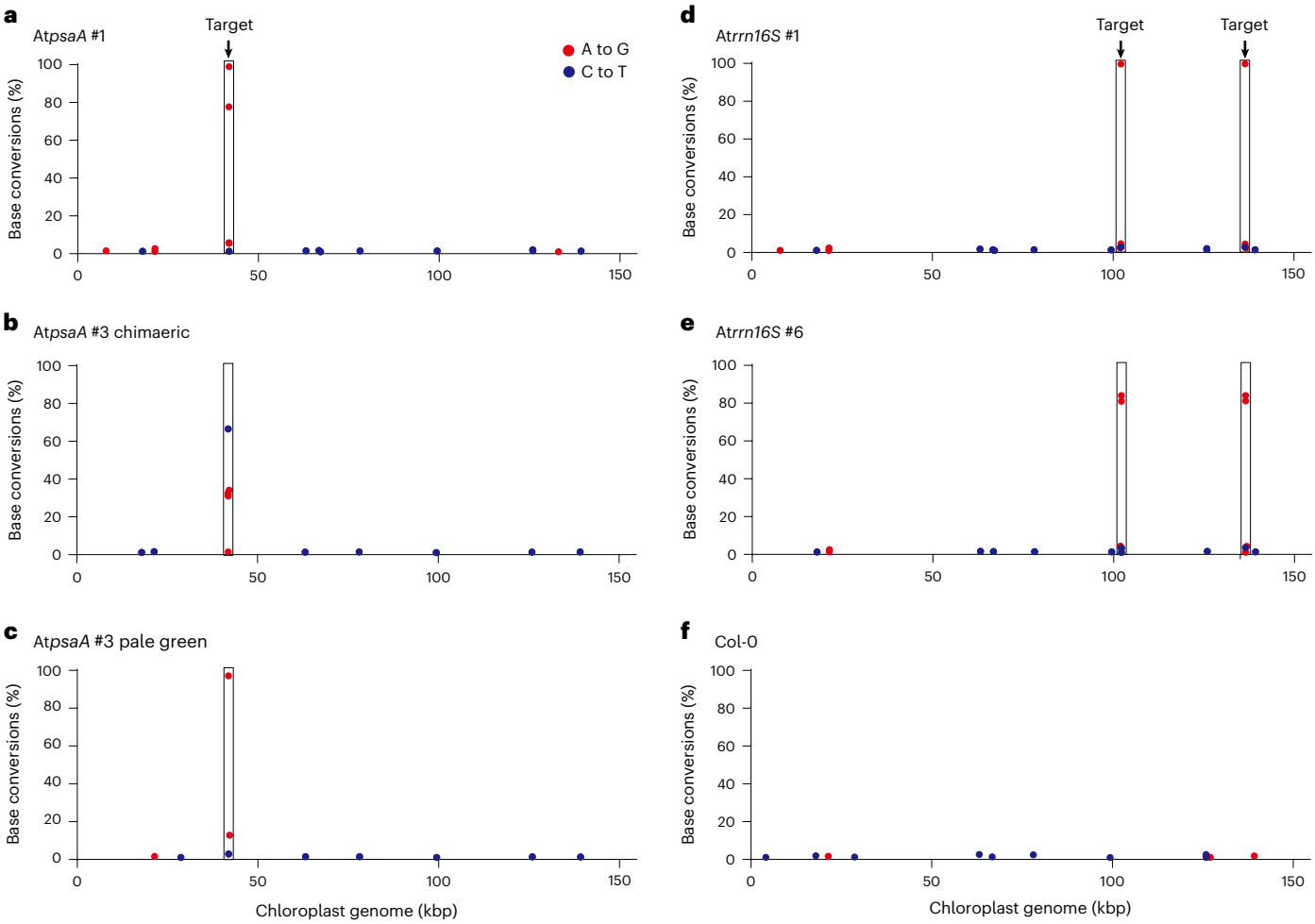


**Fig. 4 | Analysis of TALED-induced off-target effects in the *Arabidopsis* plastid genome. a–f**, Chloroplast-genome-wide plots showing A-to-G or C-to-T base conversions relative to the reference genome (AP000423.1). We analysed *psaA*-edited (**a**–**c**) and *rrn16S*-edited (**d**,**e**) T1 plants in addition to Col-0 (**f**). Note that there are two identical target sites for the *rrn16S*-specific TALED. kbp, kilobases.

frequencies that ranged from 1.0% to 4.4% in the chloroplast genome. Most of these single-nucleotide conversions, relative to the reference chloroplast genome, were also observed in the negative control (Col-0), suggesting that they represent naturally occurring heteroplasmy rather than TALED-induced off-target edits. Note also that a few of the single-nucleotide variations with low heteroplasmic fractions found in Col-0 were not detected in T1 plants or vice versa. These results show that TALEDs induce on-target edits specifically without substantial unlinked off-target mutations in cpDNA.

The TALED-mediated organellar base editing described in this study has a number of advantages over plastid transformation via homologous recombination using a targeting vector. First, organellar base editing is more broadly applicable, not limited to certain plant species amenable for plastid transformation. Second, homoplasmic editing can be achieved in a single round of *Agrobacterium*-mediated transformation, as shown in this study. In contrast, multiple rounds of marker selection and regeneration are required to obtain homoplasmy using plastid transformation. Third, no transgenes are integrated in plastid DNA with organellar base editing. In contrast, plastid transformation involves the targeted integration of a selectable marker gene into plastid DNA, which cannot be removed by breeding.

In summary, we developed plant-optimized TALEDs for A-to-G base editing in cpDNA in protoplasts and whole plants. In particular, targeted adenine editing in chloroplast genes using *Agrobacterium*-mediated transformation gave rise to heritable homoplasmic mutations, leading to phenotypic changes in *Arabidopsis*. Unlike in human mitochondrial DNA, uracil-glycosylase-inhibitor-free TALEDs catalysed C-to-T (in addition to A-to-G) conversions at some but not all positions in the context of a 5′-TC-3′ motif in cpDNA. It will be important to investigate whether TALEDs yield different editing outcomes in mammalian mitochondria and in plant chloroplasts, possibly because of the differences in mismatch DNA repair systems, and to develop TALEDs catalysing A-to-G conversions exclusively (without C-to-T conversions) in plants. TALEDs, together with DddA-derived cytosine base editors, can now induce targeted A-to-G and C-to-T base editing in plant organellar DNA, which could pave the way for enhancing the efficiency of photosynthesis and $CO_2$ fixation in plants, contributing to agricultural innovations and carbon neutralization.

## Methods

### Plasmid construction

TALE arrays were designed to target *rrn16S*, *psaA*, *psbA* and *rbcL* following the approach used in previous reports[4,5,10,13,19]. PCR amplicons encoding the TALE array, $DddA_{tox}$ split and ABE8e, generated using PrimeSTAR GXL DNA Polymerase (TAKARA), were cloned into pRPS5A–CTS digested with SmaI and KpnI (NEB) using Gibson assembly (NEB). Specifically, the left-side and right-side TALED sequences were cloned into pRPS5A–CTS–35S terminator–AatII–PmeI vector and AatII–pRPS5A–CTS–35S terminator–PmeI, respectively. The left-side and right-side TALED constructs were transcribed in vitro, and the resulting

mRNAs were used for lettuce protoplast transfection. For *Arabidopsis* transformation, the left and right TALED vectors were digested with AatII and PmeI (NEB) and ligated using T4 DNA ligase (NEB) (Extended Data Fig. 2). The assembled plasmids were chemically transformed into *E. coli* DH5α, and plasmids from the surviving colonies were analysed by the Sanger sequencing method. The TALE binding sequences are listed in Supplementary Table 1. The primers for PCR amplification are listed in Supplementary Table 2. The plasmids used in this study and their annotated DNA sequences are available from Addgene (ID 189639–189652).

### Lettuce protoplast isolation and transfection

Lettuce (*Lactuca sativa* cv. Cheongchima) seeds were sterilized by immersing them in 70% ethanol for 30 s and then in a 0.4% hypochlorite solution for 15 min prior to washing them three times in distilled water. The sterilized lettuce seeds were germinated on half-strength MS medium supplemented with 2% sucrose at 25 °C under 16 h of light and 8 h of dark. Protoplast isolation and transfection were performed as described in a previous report[10].

### mRNA in vitro transcription

For use as in vitro transcription templates, DNA templates were amplified using PrimeSTAR GXL DNA Polymerase (TAKARA). The mRNAs were synthesized and purified using an in vitro mRNA synthesis kit (Enzynomics). We used 40 μg of each type of transcript for protoplast transfection. The primers for DNA template PCR amplification are listed in Supplementary Table 2.

### Plant transformation and transformant selection

*A. thaliana* Columbia-0 (Col-0) plants were transformed by floral dipping with *Agrobacterium tumefaciens* strain GV3101 as described in a previous report[20]. After transformation, *Arabidopsis* T1 seeds were plated on half-strength MS medium containing 1% sucrose, 20 mg $l^{-1}$ phosphinothricin and 250 mg $l^{-1}$ cefataxim. All transgenic plants were grown at 23 °C under long-day conditions (16 h of light and 8 h of dark).

### Targeted deep sequencing

Total DNA was isolated from cultured cells at day 7 post-transfection[10] and true leaves from selected plants using a DNeasy Plant Mini kit (Qiagen). On-target sites were amplified through a primary PCR, a secondary PCR and a third PCR to generate deep sequencing libraries using TruSeq HT Dual index-containing primers and PrimeSTAR GXL DNA Polymerase (TAKARA). Illumina MiniSeq paired-end sequencing systems were used to sequence the libraries. The base editing frequencies are presented as percentages of sequencing reads containing base conversions among total sequencing reads. The program used to analyse the frequency of edits is available at https://github.com/ibs-cge/maund. The PCR primer sequences are shown in Supplementary Tables 3 and 4.

### Genotyping of T2 plants

Total DNAs were isolated from true leaves from T2 plants using a DNeasy Plant Mini kit (Qiagen). The regions of interest were amplified from total DNAs using PrimeSTAR GXL DNA Polymerase (TAKARA), after which the PCR amplicons were analysed on a 1% agarose gel. The PCR primer sequences are shown in Supplementary Tables 2 and 4.

### Next-generation sequencing

For analysis of off-target effects, single nucleotide polymorphisms were called in the plastid genomes using sequencing data from total DNA. First, paired-end libraries were prepared from total DNA using a TruSeq DNA PCR-Free Kit (Illumina) for At*psa* #1 and At*rrn16S* #1 and #6 and a TruSeq Nano DNA Kit (Illumina) for At*psa* #3 (chimaeric and pale-green leaf samples) and Col-0. Sequencing was performed with an Illumina HiSeq X Ten platform. To analyse the next-generation sequencing data from whole-chloroplast-genome sequencing, we followed the methods in a previously published report[11]. Paired-end reads were mapped to reference sequences (AP000423.1) using BWA (v.0.7.17) (ref. [21]) in single-ended mode. We filtered out mapped reads with mapping identities ≤99%. Single nucleotide polymorphisms were then called using pysam (v.0.18.0) (ref. [22]). Finally, we listed the positions of variants with A-to-G and C-to-T conversion rates ≥1% with read depths ≥5,000.

### Reporting summary

Further information on research design is available in the Nature Portfilio Reporting Summary linked to this article.

## Data availability

The DNA sequencing data have been deposited in the National Center for Biotechnology Information (NCBI) Sequence Read Archive (SRA) database with BioProject accession code PRJNA858174. The protein sequences of the TALE arrays and TadA-8e are provided in the Supplementary Information. Any other additional data are available in the Supplementary Information. Source data are provided with this paper.

## Code availability

Source code (https://github.com/ibs-cge/maund, created by BotBot Inc.) was used to calculate base editing frequencies from targeted deep sequencing data.

## References


1. Dobrogojski, J., Adamiec, M. & Lucinski, R. The chloroplast genome: a review. *Acta Physiol. Plant* **42**, 98 (2020).
2. Gammage, P. A., Moraes, C. T. & Minczuk, M. Mitochondrial genome engineering: the revolution may not be CRISPR-ized. *Trends Genet.* **34**, 101–110 (2018).
3. Mok, B. Y. et al. A bacterial cytidine deaminase toxin enables CRISPR-free mitochondrial base editing. *Nature* **583**, 631–637 (2020).
4. Mok, Y. G. et al. Base editing in human cells with monomeric DddA–TALE fusion deaminases. *Nat. Commun.* **13**, 4038 (2022).
5. Lee, H. et al. Mitochondrial DNA editing in mice with DddA–TALE fusion deaminases. *Nat. Commun.* **12**, 1190 (2021).
6. Guo, J. et al. DdCBE mediates efficient and inheritable modifications in mouse mitochondrial genome. *Mol. Ther. Nucleic Acids* **27**, 73–80 (2021).
7. Silva-Pinheiro, P. et al. In vivo mitochondrial base editing via adeno-associated viral delivery to mouse post-mitotic tissue. *Nat. Commun.* **13**, 750 (2022).
8. Mok, B. Y. et al. CRISPR-free base editors with enhanced activity and expanded targeting scope in mitochondrial and nuclear DNA. *Nat. Biotechnol.* **40**, 1378–1387 (2022).
9. Lim, K. et al. Nuclear and mitochondrial DNA editing in human cells with zinc finger deaminases. *Nat. Commun.* **13**, 366 (2022).
10. Kang, B.-C. et al. Chloroplast and mitochondrial DNA editing in plants. *Nat. Plants* **7**, 899–905 (2021).
11. Nakazato, I. et al. Targeted base editing in the plastid genome of *Arabidopsis thaliana*. *Nat. Plants* **7**, 906–913 (2021).
12. Li, R. et al. High-efficiency plastome base editing in rice with TAL cytosine deaminase. *Mol. Plant* **14**, 1412–1414 (2021).
13. Cho, S.-I. et al. Targeted A-to-G base editing in human mitochondrial DNA with programmable deaminases. *Cell* **185**, 1764–1776 (2022).
14. Miyazaki, K. & Kitahara, K. Functional metagenomic approach to identify overlooked antibiotic resistance mutations in bacterial rRNA. *Sci. Rep.* **8**, 5179 (2018).
15. Narusaka, Y., Narusaka, M., Kobayashi, H. & Satoh, K. The herbicide-resistant species of the cyanobacterial Dl protein obtained by thorough and random in vitro mutagenesis. *Plant Cell Physiol.* **39**, 620–626 (1998).

16. Weijers, D. et al. An *Arabidopsis* Minute-like phenotype caused by a semi-dominant mutation in a RIBOSOMAL PROTEIN S5 gene. *Development* **128**, 4289–4299 (2001).
17. Kim, J. & Kim, J. –S. Bypassing GMO regulation with CRISPR gene editing. *Nat. Biotechnol.* **34**, 1014–1015 (2016).
18. Ishii, T. Crop gene-editing: should we bypass or apply existing GMO policy? *Trends Plant Sci.* **23**, 947–950 (2018).
19. Kim, Y. et al. A library of TAL effector nucleases spanning the human genome. *Nat. Biotechnol.* **31**, 251–258 (2013).
20. Zhang, X., Henriques, R., Lin, S. S., Niu, Q. W. & Chua, N. H. *Agrobacterium*-mediated transformation of *Arabidopsis thaliana* using the floral dip method. *Nat. Protoc.* **1**, 641–646 (2006).
21. Li, H. & Durbin, R. Fast and accurate short read alignment with Burrows–Wheeler transform. *Bioinformatics* **25**, 1754–1760 (2009).
22. Gilman P. et al. PySAM (Python Wrapper for System Advisor Model "SAM") https://doi.org/10.11578/dc.20190903.1 (2019).

## Acknowledgements

This work was supported by the Institute for Basic Science (grant no. IBS-R021-D1-a00 to J.-S.K.).

## Author contributions

Y.G.M., S.H. and J.-S.K. designed the study. Y.G.M., S.H., S.-J.B. and S.-I.C. performed the experiments. Y.G.M., S.H. and J.-S.K. wrote the manuscript. J.-S.K. supervised the research.

## Competing interests

A provisional patent application was submitted based on the results reported in this paper. J.-S.K. is a founder of and shareholder in ToolGen.

## Additional information

**Extended data** is available for this paper at https://doi.org/10.1038/s41477-022-01279-8.

**Supplementary information** The online version contains supplementary material available at https://doi.org/10.1038/s41477-022-01279-8.

**Correspondence and requests for materials** should be addressed to Jin-Soo Kim.

**Peer review information** *Nature Plants* thanks Yiping Qi and the other, anonymous, reviewer(s) for their contribution to the peer review of this work.

https://doi.org/10.1038/s41477-022-01279-8

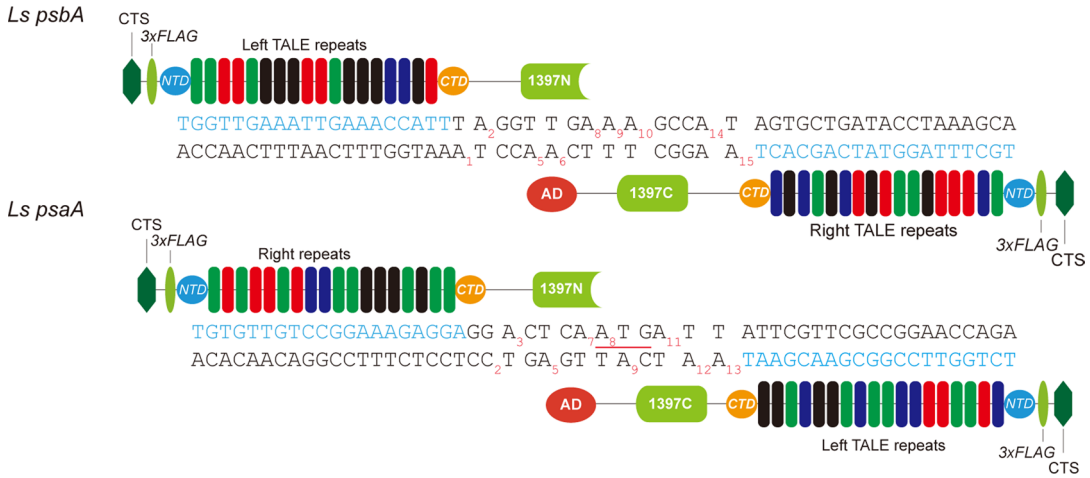


**Extended Data Fig. 1 | TALED pairs designed to target *psbA* and *psaA* chloroplast genes in lettuce.** The TALE-binding sites are shown in blue. CTS, Chloroplasts target signal; NTD, N-terminal domain; CTD, C-terminal domain, 1397 N and 1397 C, split $DddA_{tox}$ half; AD, adenine deaminase (ABE8e).

https://doi.org/10.1038/s41477-022-01279-8

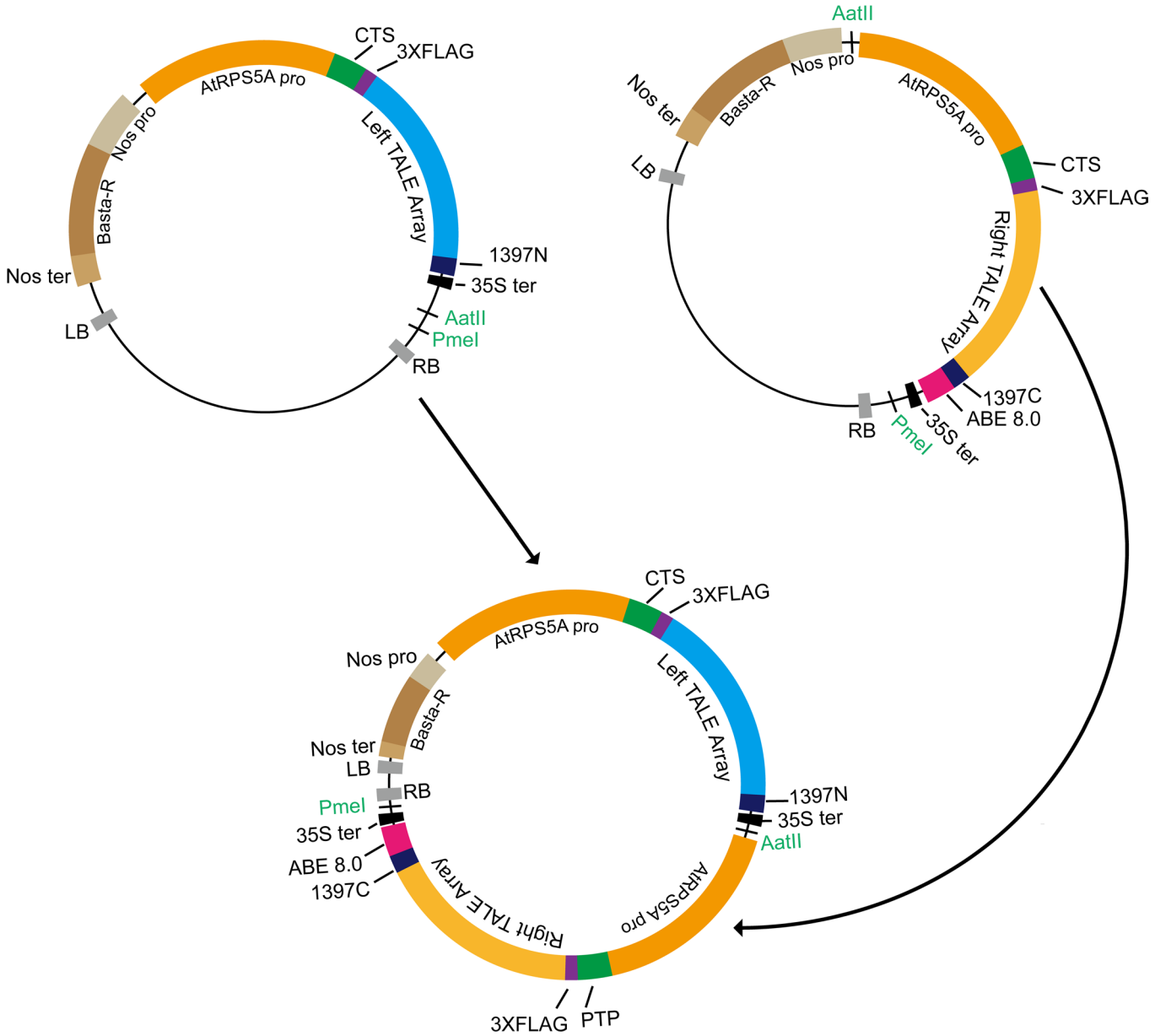


**Extended Data Fig. 2 | TALED of chloroplast target constructs assembly schematic.** Each TALED pairs were cloned into a different T-vector: Left TALE(L-1397N) cloned into RPS5A$_{pro}$-CTS-35S$_{ter}$-Aat II-Pme I T-vector and Right TALE (R-1397C-AD) cloned into Aat II-RPS5A$_{pro}$- CTS-35S$_{ter}$-PmeI. After digesting each vector with Aat II and Pme I, Aat II-RPS5A$_{pro}$-CTS-Right TALE-1397C-AD-35S$_{ter}$-PmeI was ligated to a vector with pRPS5A$_{pro}$-CTS-Left TALE-1397N-35S$_{ter}$-Aat II-Pme I, and the TALED pair was cloned into one vector. 1397 N and 1397C-ABE8.0 (ABE8e), which intersected in Left TALE and Right TALE, were also constructed.

https://doi.org/10.1038/s41477-022-01279-8

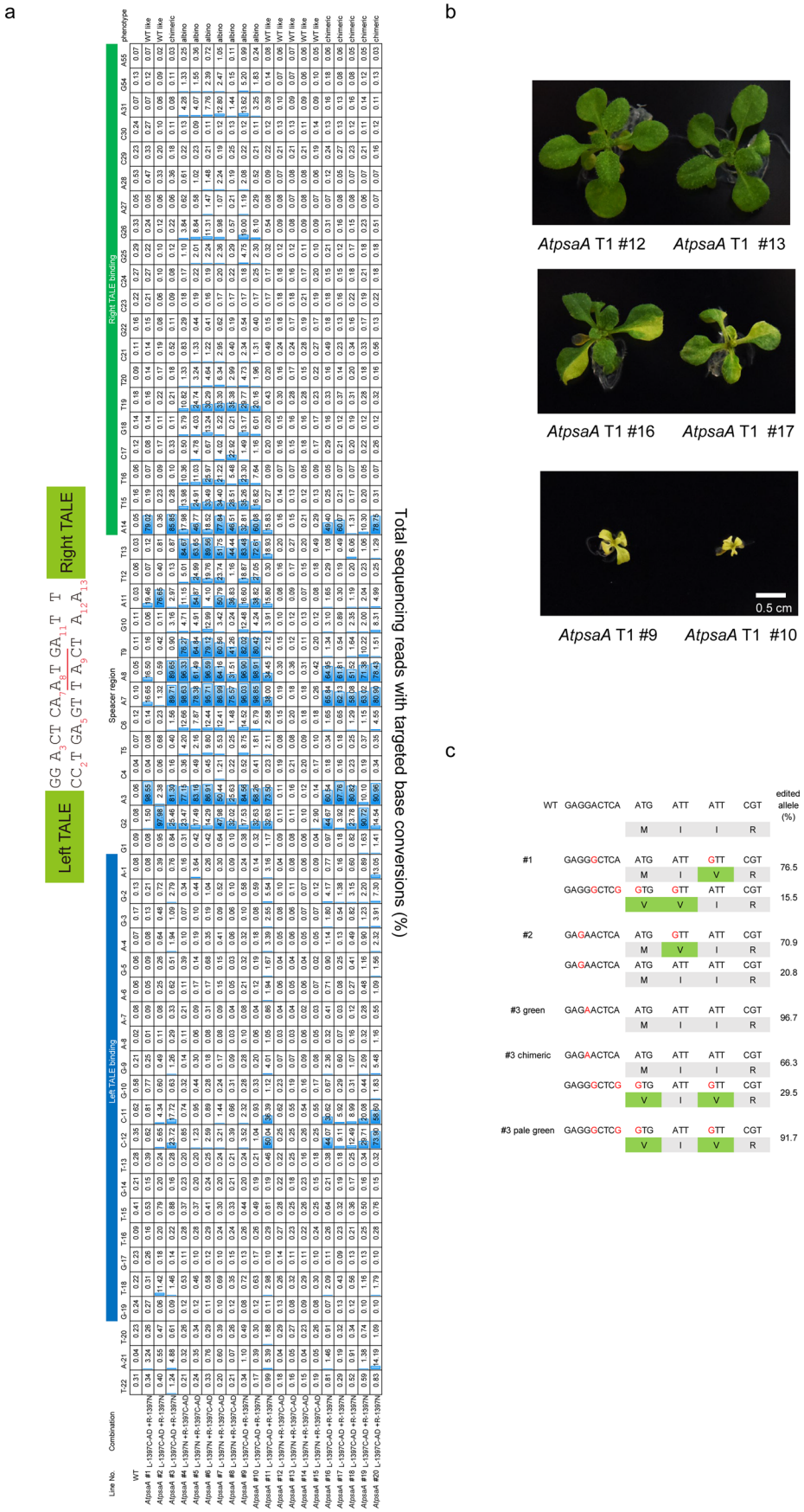


**Extended Data Fig. 3 | Analysis of *AtpsaA* T1 plants.** Editing frequencies (a) and phenotypes (b) and allele frequencies (c) of *psaA* targeted T1 plants. The TALE binding regions are shown in green, and analyzed nucleotides are shown in numbers. The adenine of the desired target for base editing is indicated in red underline. Edited bases were represented by red (c). The base conversion rates were measured by targeted deep sequencing.

https://doi.org/10.1038/s41477-022-01279-8

a

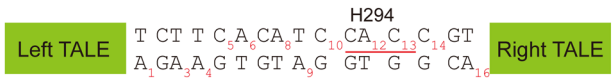


| Line No. | Combination | A-4 | A-3 | C-2 | A-1 | A1 | C2 | A3 | A4 | C5 | A6 | C7 | A8 | A9 | C10 | C11 | A12 | C13 | C14 | C15 | A16 | C17 | C18 | phenotype |
|---|---|---|---|---|---|---|---|---|---|---|---|---|---|---|---|---|---|---|---|---|---|---|---|---|
| WT | | 0.03 | 0.06 | 0.06 | 0.04 | 0.07 | 0.04 | 0.17 | 0.03 | 0.05 | 0.04 | 0.04 | 0.09 | 0.05 | 0.04 | 0.07 | 0.20 | 0.04 | 0.06 | 0.09 | 0.07 | 0.07 | 0.10 | |
| AtrbcL H294 #1 | L-1397N +R-1397C-AD | 3.31 | 31.81 | 0.06 | 0.29 | 0.82 | 0.17 | 1.64 | 2.21 | 1.06 | 3.79 | 0.00 | 84.35 | 95.50 | 1.15 | 0.15 | 79.63 | 0.49 | 1.87 | 1.49 | 92.80 | 0.28 | 0.28 | Chimeric |
| AtrbcL H294 #2 | L-1397N +R-1397C-AD | 3.90 | 3.64 | 0.10 | 0.21 | 0.41 | 0.17 | 0.70 | 1.30 | 1.62 | 1.80 | 0.04 | 4.59 | 96.56 | 1.17 | 0.35 | 5.01 | 4.21 | 4.57 | 0.70 | 31.29 | 0.17 | 0.29 | Chimeric |
| AtrbcL H294 #3 | L-1397C-AD +R-1397N | 0.08 | 0.04 | 0.05 | 0.01 | 0.05 | 0.05 | 0.19 | 0.05 | 0.06 | 0.19 | 0.06 | 0.30 | 96.63 | 0.07 | 0.04 | 0.35 | 0.03 | 0.10 | 0.09 | 32.18 | 0.10 | 0.08 | Chimeric |
| AtrbcL H294 #4 | L-1397C-AD +R-1397N | 0.15 | 0.52 | 0.06 | 0.08 | 0.13 | 0.08 | 0.24 | 0.31 | 0.55 | 1.59 | 0.06 | 19.69 | 97.93 | 0.08 | 0.12 | 17.04 | 0.27 | 0.30 | 0.06 | 97.82 | 0.11 | 0.06 | Chimeric |
| AtrbcL H294 #5 | L-1397C-AD +R-1397N | 0.07 | 3.09 | 0.04 | 0.05 | 0.05 | 0.04 | 0.19 | 3.00 | 0.16 | 0.56 | 0.05 | 39.67 | 99.31 | 0.06 | 0.03 | 0.69 | 0.24 | 0.29 | 0.11 | 54.59 | 0.12 | 0.04 | Chimeric |
| AtrbcL H294 #6 | L-1397C-AD +R-1397N | 2.04 | 76.02 | 0.08 | 0.10 | 0.23 | 0.12 | 0.39 | 0.95 | 0.71 | 0.62 | 0.09 | 2.91 | 83.60 | 0.40 | 0.12 | 75.59 | 0.37 | 0.68 | 0.31 | 98.16 | 0.11 | 0.09 | Chimeric |

Total sequencing reads with targeted base conversions (%)

b


**Extended Data Fig. 4 | Analysis of *AtrbcL* T1 plants.** Editing frequencies (a) and allele frequencies (b) of *rbcL* targeted T1 plants. The TALE binding regions are shown in green, and analyzed nucleotides are shown in numbers. The adenine of the desired target for base editing is indicated in red underline. Edited bases were represented by red (b). The base conversion rates were measured by targeted deep sequencing.

https://doi.org/10.1038/s41477-022-01279-8


| Line No. | Combination | A-3 | C-2 | A-1 | C1 | C2 | A3 | C4 | A5 | A6 | C7 | C8 | A9 | C10 | A11 | C12 | C13 | A14 | A15 |
|---|---|---|---|---|---|---|---|---|---|---|---|---|---|---|---|---|---|---|---|
| WT | | 0.06 | 0.09 | 0.26 | 0.11 | 0.10 | 0.12 | 0.14 | 0.09 | 0.13 | 0.10 | 0.13 | 0.21 | 0.08 | 0.10 | 0.16 | 0.07 | 0.06 | 0.07 |
| *Atrn16S* #1 | L-1397N +R-1397C-AD | 0.06 | 1.23 | 0.30 | 0.09 | 0.12 | 0.25 | 0.68 | 15.21 | 98.40 | 0.46 | 0.09 | 99.30 | 0.12 | 0.18 | 0.28 | 0.23 | 0.08 | 0.07 |
| *Atrn16S* #2 | L-1397N +R-1397C-AD | 0.17 | 2.33 | 0.45 | 0.10 | 0.18 | 0.28 | 0.65 | 0.20 | 1.98 | 0.91 | 0.25 | 67.36 | 0.41 | 0.14 | 0.44 | 0.33 | 0.08 | 0.10 |
| *Atrn16S* #3 | L-1397N +R-1397C-AD | 0.08 | 1.43 | 0.33 | 0.08 | 0.11 | 0.12 | 0.27 | 0.20 | 1.02 | 0.23 | 0.18 | 1.66 | 0.71 | 0.28 | 0.17 | 0.13 | 0.07 | 0.05 |
| *Atrn16S* #4 | L-1397N +R-1397C-AD | 0.05 | 0.20 | 0.47 | 0.11 | 0.10 | 0.18 | 0.23 | 0.31 | 99.75 | 0.09 | 0.10 | 99.70 | 0.10 | 0.14 | 0.11 | 0.09 | 0.07 | 0.07 |
| *Atrn16S* #5 | L-1397N +R-1397C-AD | 0.19 | 29.02 | 0.40 | 0.10 | 0.15 | 0.15 | 0.47 | 0.17 | 1.81 | 0.47 | 0.18 | 46.10 | 0.39 | 0.18 | 0.27 | 0.16 | 0.07 | 0.07 |
| *Atrn16S* #6 | L-1397N +R-1397C-AD | 0.08 | 2.89 | 0.31 | 0.09 | 0.10 | 0.19 | 0.38 | 0.22 | 4.35 | 0.35 | 0.16 | 99.76 | 0.09 | 96.25 | 0.09 | 0.11 | 0.07 | 0.08 |
| *Atrn16S* #7 | L-1397N +R-1397C-AD | 0.43 | 5.15 | 0.90 | 0.10 | 0.24 | 0.34 | 1.14 | 0.67 | 10.21 | 1.16 | 0.28 | 99.42 | 0.15 | 1.22 | 0.76 | 0.56 | 0.08 | 0.11 |
| *Atrn16S* #8 | L-1397N +R-1397C-AD | 1.20 | 97.75 | 0.46 | 0.09 | 0.18 | 0.36 | 0.94 | 0.23 | 5.57 | 0.94 | 0.32 | 98.38 | 0.27 | 0.26 | 0.57 | 0.45 | 0.07 | 0.06 |
| *Atrn16S* #9 | L-1397N +R-1397C-AD | 0.38 | 19.10 | 0.40 | 0.06 | 0.35 | 0.22 | 0.53 | 0.27 | 3.50 | 0.82 | 0.22 | 46.51 | 1.64 | 0.16 | 0.26 | 0.20 | 0.08 | 0.11 |
| *Atrn16S* #10 | L-1397N +R-1397C-AD | 0.16 | 29.20 | 0.38 | 0.11 | 0.09 | 0.11 | 0.14 | 0.11 | 0.73 | 0.18 | 0.12 | 62.08 | 0.23 | 0.14 | 0.11 | 0.11 | 0.05 | 0.06 |
| *Atrn16S* #11 | L-1397N +R-1397C-AD | 0.15 | 2.39 | 0.38 | 0.08 | 0.11 | 0.17 | 0.69 | 0.21 | 1.45 | 0.73 | 0.19 | 36.73 | 1.55 | 0.18 | 0.24 | 0.21 | 0.06 | 0.05 |
| *Atrn16S* #12 | L-1397N +R-1397C-AD | 0.33 | 4.48 | 0.48 | 0.13 | 0.16 | 0.22 | 0.62 | 0.32 | 3.16 | 0.69 | 0.22 | 5.86 | 1.47 | 0.28 | 0.32 | 0.24 | 0.06 | 0.05 |
| *Atrn16S* #13 | L-1397N +R-1397C-AD | 0.23 | 1.70 | 0.35 | 0.09 | 0.16 | 7.22 | 0.62 | 0.32 | 44.59 | 0.38 | 0.15 | 80.37 | 0.31 | 0.20 | 0.40 | 0.32 | 0.07 | 0.06 |
| *Atrn16S* #14 | L-1397N +R-1397C-AD | 0.22 | 2.61 | 0.25 | 0.10 | 0.13 | 0.31 | 0.28 | 0.20 | 46.74 | 0.32 | 0.11 | 4.32 | 0.70 | 0.18 | 0.21 | 0.14 | 0.12 | 0.07 |
| *Atrn16S* #15 | L-1397N +R-1397C-AD | 0.18 | 4.57 | 0.34 | 0.08 | 0.13 | 0.22 | 0.61 | 0.20 | 2.32 | 0.65 | 0.20 | 56.63 | 1.03 | 0.20 | 0.27 | 0.21 | 0.06 | 0.09 |
| *Atrn16S* #16 | L-1397N +R-1397C-AD | 0.49 | 4.88 | 0.51 | 0.11 | 0.28 | 0.46 | 0.95 | 0.33 | 4.12 | 1.10 | 0.25 | 5.83 | 2.23 | 0.26 | 0.34 | 0.27 | 0.12 | 0.08 |
| *Atrn16S* #17 | L-1397N +R-1397C-AD | 0.10 | 2.14 | 0.41 | 0.10 | 0.13 | 0.18 | 0.50 | 0.15 | 2.18 | 0.44 | 0.13 | 54.74 | 0.57 | 0.49 | 0.23 | 0.15 | 0.08 | 0.05 |
| *Atrn16S* #18 | L-1397C-AD +R-1397N | 0.04 | 0.07 | 0.26 | 0.15 | 0.09 | 0.12 | 0.11 | 0.16 | 0.14 | 0.13 | 0.14 | 0.19 | 0.11 | 0.12 | 0.07 | 0.07 | 0.04 | 0.06 |
| *Atrn16S* #19 | L-1397C-AD +R-1397N | 0.08 | 0.14 | 0.22 | 0.11 | 0.15 | 0.27 | 0.26 | 0.14 | 3.08 | 0.12 | 0.13 | 99.77 | 0.14 | 0.16 | 0.39 | 0.47 | 0.24 | 0.94 |
| *Atrn16S* #20 | L-1397N +R-1397C-AD | 0.81 | 8.30 | 6.49 | 0.07 | 0.29 | 0.61 | 0.84 | 59.46 | 81.99 | 0.13 | 0.02 | 8.17 | 2.15 | 0.63 | 0.47 | 0.39 | 0.14 | 0.09 |
| *Atrn16S* #21 | L-1397N +R-1397C-AD | 0.13 | 9.05 | 0.27 | 0.11 | 0.14 | 0.19 | 0.42 | 27.55 | 31.19 | 0.43 | 0.11 | 93.12 | 0.13 | 0.25 | 0.24 | 0.14 | 0.09 | 0.10 |
| *Atrn16S* #22 | L-1397N +R-1397C-AD | 0.47 | 49.69 | 0.27 | 0.07 | 0.22 | 0.45 | 0.78 | 0.20 | 4.55 | 0.63 | 0.13 | 51.29 | 0.95 | 0.23 | 0.29 | 0.28 | 0.15 | 0.09 |
| *Atrn16S* #23 | L-1397N +R-1397C-AD | 0.16 | 1.82 | 0.24 | 0.06 | 0.16 | 0.20 | 0.40 | 0.21 | 1.65 | 0.38 | 0.14 | 3.58 | 0.81 | 0.18 | 0.13 | 0.12 | 0.05 | 0.05 |
| *Atrn16S* #24 | L-1397N +R-1397C-AD | 0.12 | 0.91 | 0.23 | 0.10 | 0.14 | 0.20 | 0.21 | 0.19 | 1.29 | 0.18 | 0.06 | 98.67 | 0.07 | 0.17 | 0.09 | 0.10 | 0.06 | 0.06 |
| *Atrn16S* #25 | L-1397N +R-1397C-AD | 0.16 | 2.40 | 0.18 | 0.08 | 0.15 | 0.21 | 0.38 | 0.30 | 2.31 | 0.40 | 0.10 | 3.25 | 0.88 | 0.21 | 0.10 | 0.10 | 0.06 | 0.04 |
| *Atrn16S* #26 | L-1397N +R-1397C-AD | 0.23 | 2.37 | 0.21 | 0.05 | 0.20 | 0.26 | 0.32 | 0.18 | 2.42 | 0.25 | 0.06 | 3.49 | 0.58 | 0.26 | 0.08 | 0.10 | 0.14 | 0.09 |
| *Atrn16S* #27 | L-1397N +R-1397C-AD | 0.31 | 4.46 | 0.40 | 0.06 | 0.18 | 0.49 | 0.82 | 0.36 | 5.58 | 0.90 | 0.19 | 46.97 | 0.88 | 0.34 | 0.34 | 0.32 | 0.09 | 0.08 |
| *Atrn16S* #28 | L-1397N +R-1397C-AD | 0.19 | 2.72 | 0.30 | 0.07 | 0.18 | 0.30 | 0.33 | 0.19 | 2.25 | 0.33 | 0.07 | 3.92 | 0.76 | 0.22 | 0.13 | 0.12 | 0.08 | 0.06 |
| *Atrn16S* #29 | L-1397N +R-1397C-AD | 0.21 | 2.92 | 0.41 | 0.10 | 0.18 | 0.38 | 0.71 | 0.26 | 2.64 | 0.42 | 0.08 | 22.08 | 1.16 | 0.27 | 0.19 | 0.20 | 0.09 | 0.35 |
| *Atrn16S* #30 | L-1397N +R-1397C-AD | 0.24 | 2.67 | 0.33 | 0.10 | 0.25 | 0.19 | 0.52 | 0.42 | 42.03 | 0.30 | 0.07 | 61.95 | 0.27 | 0.31 | 0.22 | 0.23 | 0.11 | 0.07 |
| *Atrn16S* #31 | L-1397N +R-1397C-AD | 0.11 | 1.00 | 0.19 | 0.12 | 0.13 | 0.26 | 0.13 | 0.18 | 1.84 | 0.16 | 0.07 | 27.69 | 0.28 | 0.19 | 0.05 | 0.08 | 0.12 | 0.05 |
| *Atrn16S* #32 | L-1397N +R-1397C-AD | 0.14 | 1.64 | 0.24 | 0.08 | 0.15 | 0.19 | 0.28 | 0.23 | 38.12 | 0.23 | 0.04 | 55.88 | 0.39 | 20.42 | 0.10 | 0.10 | 0.09 | 0.05 |
| *Atrn16S* #33 | L-1397N +R-1397C-AD | 0.13 | 17.22 | 0.16 | 0.04 | 0.15 | 0.19 | 0.23 | 0.14 | 0.77 | 0.30 | 0.07 | 18.64 | 0.44 | 0.23 | 0.16 | 0.07 | 0.04 | 0.08 |
| *Atrn16S* #34 | L-1397N +R-1397C-AD | 0.14 | 3.17 | 0.18 | 0.09 | 0.17 | 0.36 | 0.25 | 0.23 | 1.74 | 0.32 | 0.08 | 3.94 | 1.07 | 0.26 | 0.10 | 0.12 | 0.06 | 0.03 |
| *Atrn16S* #35 | L-1397C-AD +R-1397N | 0.07 | 0.17 | 0.21 | 0.08 | 0.09 | 0.15 | 0.04 | 0.21 | 0.06 | 0.04 | 0.03 | 0.23 | 0.04 | 0.24 | 0.03 | 0.05 | 0.07 | 0.06 |
| *Atrn16S* #36 | L-1397C-AD +R-1397N | 0.09 | 0.18 | 0.15 | 0.10 | 0.21 | 0.88 | 0.66 | 1.57 | 4.29 | 0.22 | 0.07 | 98.50 | 0.10 | 0.71 | 1.71 | 2.65 | 1.33 | 3.31 |
| *Atrn16S* #37 | L-1397C-AD +R-1397N | 0.05 | 0.25 | 0.17 | 0.08 | 0.22 | 0.71 | 0.39 | 0.14 | 15.11 | 0.17 | 0.05 | 99.67 | 0.24 | 89.16 | 0.04 | 0.42 | 11.56 | 4.83 |

Total sequencing reads with targeted base conversions (%)

**Extended Data Fig. 5 | Analysis of *Atrrn16S* T1 plants.** Editing frequencies of *rrn16S* targeted T1 plants. The TALE binding regions are shown in green, and analyzed nucleotides are shown in numbers. The base conversion rates were measured by targeted deep sequencing.

https://doi.org/10.1038/s41477-022-01279-8

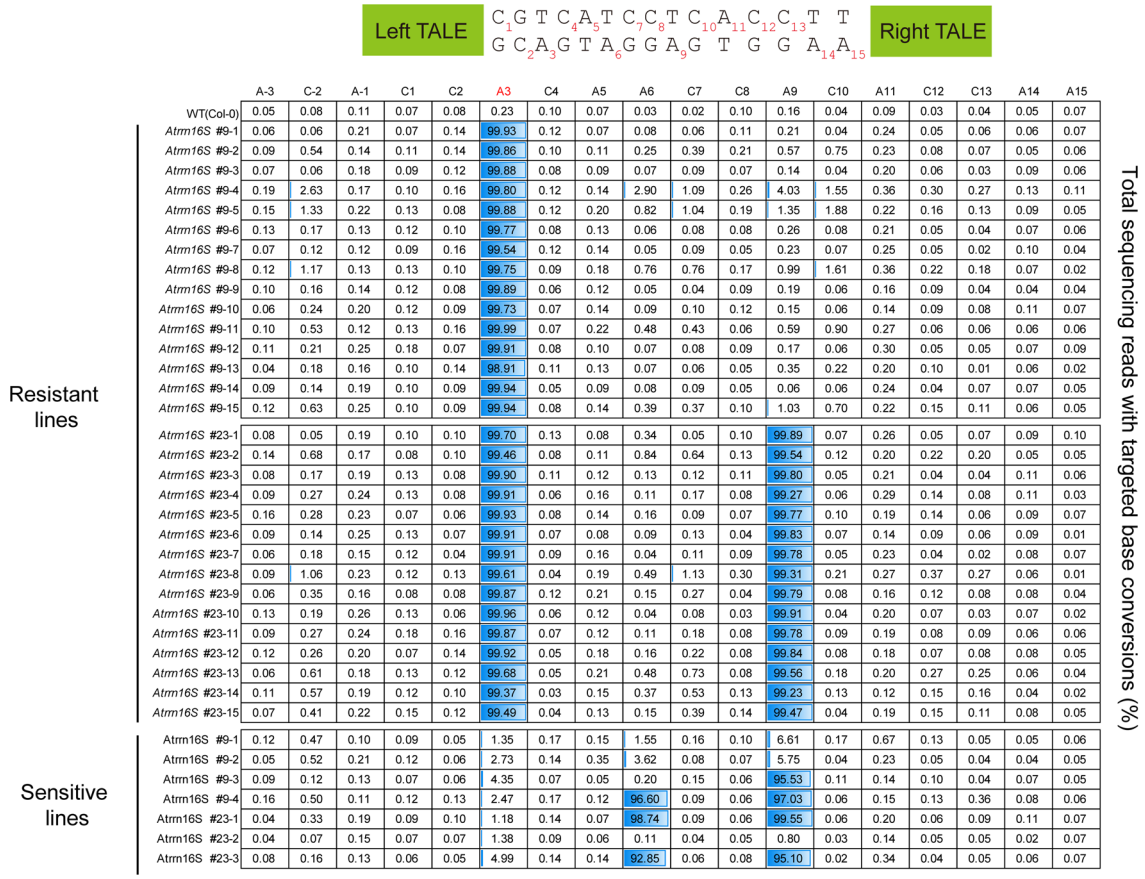


| | A-3 | C-2 | A-1 | C1 | C2 | A3 | C4 | A5 | A6 | C7 | C8 | A9 | C10 | A11 | C12 | C13 | A14 | A15 |
|---|---|---|---|---|---|---|---|---|---|---|---|---|---|---|---|---|---|---|
| WT(Col-0) | 0.05 | 0.08 | 0.11 | 0.07 | 0.08 | 0.23 | 0.10 | 0.07 | 0.03 | 0.02 | 0.10 | 0.16 | 0.04 | 0.09 | 0.03 | 0.04 | 0.05 | 0.07 |
| *Atrrn16S* #9-1 | 0.06 | 0.06 | 0.21 | 0.07 | 0.14 | 99.93 | 0.12 | 0.07 | 0.08 | 0.06 | 0.11 | 0.21 | 0.04 | 0.24 | 0.05 | 0.06 | 0.06 | 0.07 |
| *Atrrn16S* #9-2 | 0.09 | 0.54 | 0.14 | 0.11 | 0.14 | 99.86 | 0.10 | 0.11 | 0.25 | 0.39 | 0.21 | 0.57 | 0.75 | 0.23 | 0.08 | 0.07 | 0.05 | 0.06 |
| *Atrrn16S* #9-3 | 0.07 | 0.06 | 0.18 | 0.09 | 0.12 | 99.88 | 0.08 | 0.09 | 0.07 | 0.09 | 0.07 | 0.14 | 0.04 | 0.20 | 0.06 | 0.03 | 0.09 | 0.06 |
| *Atrrn16S* #9-4 | 0.19 | 2.63 | 0.17 | 0.10 | 0.16 | 99.80 | 0.12 | 0.14 | 2.90 | 1.09 | 0.26 | 4.03 | 1.55 | 0.36 | 0.30 | 0.27 | 0.13 | 0.11 |
| *Atrrn16S* #9-5 | 0.15 | 1.33 | 0.22 | 0.13 | 0.08 | 99.88 | 0.12 | 0.20 | 0.82 | 1.04 | 0.19 | 1.35 | 1.88 | 0.22 | 0.16 | 0.13 | 0.09 | 0.05 |
| *Atrrn16S* #9-6 | 0.13 | 0.17 | 0.13 | 0.12 | 0.10 | 99.77 | 0.08 | 0.13 | 0.06 | 0.08 | 0.08 | 0.26 | 0.08 | 0.21 | 0.05 | 0.04 | 0.07 | 0.06 |
| *Atrrn16S* #9-7 | 0.07 | 0.12 | 0.12 | 0.09 | 0.16 | 99.54 | 0.12 | 0.14 | 0.05 | 0.09 | 0.05 | 0.23 | 0.07 | 0.25 | 0.05 | 0.02 | 0.10 | 0.04 |
| *Atrrn16S* #9-8 | 0.12 | 1.17 | 0.13 | 0.13 | 0.10 | 99.75 | 0.09 | 0.18 | 0.76 | 0.76 | 0.17 | 0.99 | 1.61 | 0.36 | 0.22 | 0.18 | 0.07 | 0.02 |
| *Atrrn16S* #9-9 | 0.10 | 0.16 | 0.14 | 0.12 | 0.08 | 99.89 | 0.06 | 0.12 | 0.05 | 0.04 | 0.09 | 0.19 | 0.06 | 0.16 | 0.09 | 0.04 | 0.04 | 0.04 |
| *Atrrn16S* #9-10 | 0.06 | 0.24 | 0.20 | 0.12 | 0.09 | 99.73 | 0.07 | 0.14 | 0.09 | 0.10 | 0.12 | 0.15 | 0.06 | 0.14 | 0.09 | 0.08 | 0.11 | 0.07 |
| *Atrrn16S* #9-11 | 0.10 | 0.53 | 0.12 | 0.13 | 0.16 | 99.99 | 0.07 | 0.22 | 0.48 | 0.43 | 0.06 | 0.59 | 0.90 | 0.27 | 0.06 | 0.06 | 0.06 | 0.06 |
| *Atrrn16S* #9-12 | 0.11 | 0.21 | 0.25 | 0.18 | 0.07 | 99.91 | 0.08 | 0.10 | 0.07 | 0.08 | 0.09 | 0.17 | 0.06 | 0.30 | 0.05 | 0.05 | 0.07 | 0.09 |
| *Atrrn16S* #9-13 | 0.04 | 0.18 | 0.16 | 0.10 | 0.14 | 98.91 | 0.11 | 0.13 | 0.07 | 0.06 | 0.05 | 0.35 | 0.22 | 0.20 | 0.10 | 0.01 | 0.06 | 0.02 |
| *Atrrn16S* #9-14 | 0.09 | 0.14 | 0.19 | 0.10 | 0.09 | 99.94 | 0.05 | 0.09 | 0.08 | 0.09 | 0.05 | 0.06 | 0.06 | 0.24 | 0.04 | 0.07 | 0.07 | 0.05 |
| *Atrrn16S* #9-15 | 0.12 | 0.63 | 0.25 | 0.10 | 0.09 | 99.94 | 0.08 | 0.14 | 0.39 | 0.37 | 0.10 | 1.03 | 0.70 | 0.22 | 0.15 | 0.11 | 0.06 | 0.05 |
| *Atrrn16S* #23-1 | 0.08 | 0.05 | 0.19 | 0.10 | 0.10 | 99.70 | 0.13 | 0.08 | 0.34 | 0.05 | 0.10 | 99.89 | 0.07 | 0.26 | 0.05 | 0.07 | 0.09 | 0.10 |
| *Atrrn16S* #23-2 | 0.14 | 0.68 | 0.17 | 0.08 | 0.10 | 99.46 | 0.08 | 0.11 | 0.84 | 0.64 | 0.13 | 99.54 | 0.12 | 0.20 | 0.22 | 0.20 | 0.05 | 0.05 |
| *Atrrn16S* #23-3 | 0.08 | 0.17 | 0.19 | 0.13 | 0.08 | 99.90 | 0.11 | 0.12 | 0.13 | 0.12 | 0.11 | 99.80 | 0.05 | 0.21 | 0.04 | 0.04 | 0.11 | 0.06 |
| *Atrrn16S* #23-4 | 0.09 | 0.27 | 0.24 | 0.13 | 0.08 | 99.91 | 0.06 | 0.16 | 0.11 | 0.17 | 0.08 | 99.27 | 0.06 | 0.29 | 0.14 | 0.08 | 0.11 | 0.03 |
| *Atrrn16S* #23-5 | 0.16 | 0.28 | 0.23 | 0.07 | 0.06 | 99.93 | 0.08 | 0.14 | 0.16 | 0.09 | 0.07 | 99.77 | 0.10 | 0.19 | 0.14 | 0.06 | 0.09 | 0.07 |
| *Atrrn16S* #23-6 | 0.09 | 0.14 | 0.25 | 0.13 | 0.07 | 99.91 | 0.07 | 0.08 | 0.09 | 0.13 | 0.04 | 99.83 | 0.07 | 0.14 | 0.09 | 0.06 | 0.09 | 0.01 |
| *Atrrn16S* #23-7 | 0.06 | 0.18 | 0.15 | 0.12 | 0.04 | 99.91 | 0.09 | 0.16 | 0.04 | 0.11 | 0.09 | 99.78 | 0.05 | 0.23 | 0.04 | 0.02 | 0.08 | 0.07 |
| *Atrrn16S* #23-8 | 0.09 | 1.06 | 0.23 | 0.12 | 0.13 | 99.61 | 0.04 | 0.19 | 0.49 | 1.13 | 0.30 | 99.31 | 0.21 | 0.27 | 0.37 | 0.27 | 0.06 | 0.01 |
| *Atrrn16S* #23-9 | 0.06 | 0.35 | 0.16 | 0.08 | 0.08 | 99.87 | 0.12 | 0.21 | 0.15 | 0.27 | 0.04 | 99.79 | 0.08 | 0.16 | 0.12 | 0.08 | 0.08 | 0.04 |
| *Atrrn16S* #23-10 | 0.13 | 0.19 | 0.26 | 0.13 | 0.06 | 99.96 | 0.06 | 0.12 | 0.04 | 0.08 | 0.03 | 99.91 | 0.04 | 0.20 | 0.07 | 0.03 | 0.07 | 0.02 |
| *Atrrn16S* #23-11 | 0.09 | 0.27 | 0.24 | 0.18 | 0.16 | 99.87 | 0.07 | 0.12 | 0.11 | 0.18 | 0.08 | 99.78 | 0.09 | 0.19 | 0.08 | 0.09 | 0.06 | 0.06 |
| *Atrrn16S* #23-12 | 0.12 | 0.26 | 0.20 | 0.07 | 0.14 | 99.92 | 0.05 | 0.18 | 0.16 | 0.22 | 0.08 | 99.84 | 0.08 | 0.18 | 0.07 | 0.08 | 0.08 | 0.05 |
| *Atrrn16S* #23-13 | 0.06 | 0.61 | 0.18 | 0.13 | 0.12 | 99.68 | 0.05 | 0.21 | 0.48 | 0.73 | 0.08 | 99.56 | 0.18 | 0.20 | 0.27 | 0.25 | 0.06 | 0.04 |
| *Atrrn16S* #23-14 | 0.11 | 0.57 | 0.19 | 0.12 | 0.10 | 99.37 | 0.03 | 0.15 | 0.37 | 0.53 | 0.13 | 99.23 | 0.13 | 0.12 | 0.15 | 0.16 | 0.04 | 0.02 |
| *Atrrn16S* #23-15 | 0.07 | 0.41 | 0.22 | 0.15 | 0.12 | 99.49 | 0.04 | 0.13 | 0.15 | 0.39 | 0.14 | 99.47 | 0.04 | 0.19 | 0.15 | 0.11 | 0.08 | 0.05 |
| Atrrn16S #9-1 | 0.12 | 0.47 | 0.10 | 0.09 | 0.05 | 1.35 | 0.17 | 0.15 | 1.55 | 0.16 | 0.10 | 6.61 | 0.17 | 0.67 | 0.13 | 0.05 | 0.05 | 0.06 |
| Atrrn16S #9-2 | 0.05 | 0.52 | 0.21 | 0.12 | 0.06 | 2.73 | 0.14 | 0.35 | 3.62 | 0.08 | 0.07 | 5.75 | 0.04 | 0.23 | 0.05 | 0.04 | 0.04 | 0.05 |
| Atrrn16S #9-3 | 0.09 | 0.12 | 0.13 | 0.07 | 0.06 | 4.35 | 0.07 | 0.05 | 0.20 | 0.15 | 0.06 | 95.53 | 0.11 | 0.14 | 0.10 | 0.04 | 0.07 | 0.05 |
| Atrrn16S #9-4 | 0.16 | 0.50 | 0.11 | 0.12 | 0.13 | 2.47 | 0.17 | 0.12 | 96.60 | 0.09 | 0.06 | 97.03 | 0.06 | 0.15 | 0.13 | 0.36 | 0.08 | 0.06 |
| Atrrn16S #23-1 | 0.04 | 0.33 | 0.19 | 0.09 | 0.10 | 1.18 | 0.14 | 0.07 | 98.74 | 0.09 | 0.06 | 99.55 | 0.06 | 0.20 | 0.06 | 0.09 | 0.11 | 0.07 |
| Atrrn16S #23-2 | 0.04 | 0.07 | 0.15 | 0.07 | 0.07 | 1.38 | 0.09 | 0.06 | 0.11 | 0.04 | 0.05 | 0.80 | 0.03 | 0.14 | 0.05 | 0.05 | 0.02 | 0.07 |
| Atrrn16S #23-3 | 0.08 | 0.16 | 0.13 | 0.06 | 0.05 | 4.99 | 0.14 | 0.14 | 92.85 | 0.06 | 0.08 | 95.10 | 0.02 | 0.34 | 0.04 | 0.05 | 0.06 | 0.07 |

**Extended Data Fig. 6 | Analysis of *Atrrn16S* T2 plants.** Editing frequency of *rrn16S*-targeted T2 plants with spectinomycin (10 mg $l^{-1}$) resistance and sensitivity. The TALE binding regions are shown in green, and analyzed nucleotides are shown in numbers. The base conversion rates were measured by targeted deep sequencing.

nature portfolio

Corresponding author(s): Jin-Soo Kim

Last updated by author(s): Oct. 12, 2022

# Reporting Summary

Nature Portfolio wishes to improve the reproducibility of the work that we publish. This form provides structure for consistency and transparency in reporting. For further information on Nature Portfolio policies, see our Editorial Policies and the Editorial Policy Checklist.

## Statistics

For all statistical analyses, confirm that the following items are present in the figure legend, table legend, main text, or Methods section.

| n/a | Confirmed |
|---|---|
| ☐ | ☒ The exact sample size (*n*) for each experimental group/condition, given as a discrete number and unit of measurement |
| ☐ | ☒ A statement on whether measurements were taken from distinct samples or whether the same sample was measured repeatedly |
| ☒ | ☐ The statistical test(s) used AND whether they are one- or two-sided<br>*Only common tests should be described solely by name; describe more complex techniques in the Methods section.* |
| ☒ | ☐ A description of all covariates tested |
| ☒ | ☐ A description of any assumptions or corrections, such as tests of normality and adjustment for multiple comparisons |
| ☐ | ☒ A full description of the statistical parameters including central tendency (e.g. means) or other basic estimates (e.g. regression coefficient) AND variation (e.g. standard deviation) or associated estimates of uncertainty (e.g. confidence intervals) |
| ☒ | ☐ For null hypothesis testing, the test statistic (e.g. *F*, *t*, *r*) with confidence intervals, effect sizes, degrees of freedom and *P* value noted<br>*Give P values as exact values whenever suitable.* |
| ☒ | ☐ For Bayesian analysis, information on the choice of priors and Markov chain Monte Carlo settings |
| ☒ | ☐ For hierarchical and complex designs, identification of the appropriate level for tests and full reporting of outcomes |
| ☒ | ☐ Estimates of effect sizes (e.g. Cohen's *d*, Pearson's *r*), indicating how they were calculated |

*Our web collection on statistics for biologists contains articles on many of the points above.*

## Software and code

Policy information about availability of computer code

| | |
|---|---|
| Data collection | The MiniSeq system (Illumina) was used to perform targeted deep sequencing. The HiSeq X Ten platform (Illumina) was used whole chloroplast genome sequencing. |
| Data analysis | Source code (https://github.com/ibs-cge/maund) was used to determine based editing frequencies from targeted deep sequencing data. For data analysis and visualization, we used BWA (v.0.7.17), pysam (v0.18.0), GraphPad Prism 8, Microsoft Excel 2016, PowerPoint 2016, and Adobe Illustrator CS6. |

For manuscripts utilizing custom algorithms or software that are central to the research but not yet described in published literature, software must be made available to editors and reviewers. We strongly encourage code deposition in a community repository (e.g. GitHub). See the Nature Portfolio guidelines for submitting code & software for further information.

## Data

Policy information about availability of data

All manuscripts must include a data availability statement. This statement should provide the following information, where applicable:

- Accession codes, unique identifiers, or web links for publicly available datasets
- A description of any restrictions on data availability
- For clinical datasets or third party data, please ensure that the statement adheres to our policy

All data supporting the findings of this study are available in the paper, Extended Data and Supplementary Information. Source data are provided with this paper. DNA sequencing data were deposited in the Sequence Read Archive (SRA) database of the National Center for Biotechnology Information (NCBI) with the BioProject accession code PRJNA858174. BioProject accession code is release on Oct. 12, 2022.

# Field-specific reporting

Please select the one below that is the best fit for your research. If you are not sure, read the appropriate sections before making your selection.

☒ Life sciences ☐ Behavioural & social sciences ☐ Ecological, evolutionary & environmental sciences

For a reference copy of the document with all sections, see nature.com/documents/nr-reporting-summary-flat.pdf

# Life sciences study design

All studies must disclose on these points even when the disclosure is negative.

| | |
|---|---|
| Sample size | For transfection experiments, approximately 500,000 lettuce protoplasts were used in each experiment. At least 63 T1 plants and 37 T2 plants for each targeted genes were analyzed by targeted deep sequencing. No statistical method was used to predetermine sample size. These sample size was maximum number of plants that we could handle in the growth rooms. |
| Data exclusions | No data were excluded from the analyses. |
| Replication | The protoplasts experiments were performed from individual biological replicates (n=3). All attempts at replication were successful. |
| Randomization | Protoplast samples were randomly collected from a large pool of lettuce protoplasts for each transfection. |
| Blinding | Blinding was not required because all analyses including targeted deep sequencing and phenotyping by antibiotics and molecular methods could be carried out without making any subjective judgements. |

# Reporting for specific materials, systems and methods

We require information from authors about some types of materials, experimental systems and methods used in many studies. Here, indicate whether each material, system or method listed is relevant to your study. If you are not sure if a list item applies to your research, read the appropriate section before selecting a response.

## Materials & experimental systems

| n/a | Involved in the study |
|---|---|
| ☒ | ☐ Antibodies |
| ☒ | ☐ Eukaryotic cell lines |
| ☒ | ☐ Palaeontology and archaeology |
| ☒ | ☐ Animals and other organisms |
| ☒ | ☐ Human research participants |
| ☒ | ☐ Clinical data |
| ☒ | ☐ Dual use research of concern |

## Methods

| n/a | Involved in the study |
|---|---|
| ☒ | ☐ ChIP-seq |
| ☒ | ☐ Flow cytometry |
| ☒ | ☐ MRI-based neuroimaging |